

## **The Impact of Float Stitches on Resistance of Conductive Knitted Structures**

Su Liu, Chenxiao Yang, Yuanfang Zhao, Xiao ming Tao, Jiahui Tong and Li Li

The Hong Kong Polytechnic University, The Institute of Textiles and Clothing, Hong Kong

Corresponding author:

Li Li, The Hong Kong Polytechnic University, ST728, The Institute of Textiles and Clothing, Hunghom, Kowloon QT702, Hong Kong.

Email: li.lilly@polyu.edu.hk

### **Abstract**

Currently, conductive yarn can be knitted into fabrics to endow the traditional textile product with special attributes such as shielding electromagnetic waves, detecting and transferring electrical signals, replacing fingers in the operation of touch-screen panels, etc. Research on the electrical properties of conductive knitted fabrics can contribute to the development of such functional textiles. A few studies have been conducted, and it has been found that the variation of the knitted structure can impact the properties of a conductive knitted fabric. Among the properties of conductive fabrics, the resistance value is an important index to decide the performance of electrical functions. Several researchers have conducted practical experiments and theoretical analyses to predict the resistance of plain weft knitted structure. However, in addition to the plain weft knitted structure, the float structure is another important basic knitted structure. Therefore, a geometric model incorporated with a simplified resistive network is proposed for the calculation of the electrical resistance of conductive knitted fabrics with float stitches will be studied in this paper. The aim of the model is to determine the resistive effects of conductive float stitches on knitted structures with different numbers of knitted courses and wales. The geometric model can provide a detailed mathematical description of a single knitted loop in the Cartesian coordinate system. With the simplified resistive network, the resistance of conductive float stitches in knitted fabrics can be modelled and computed. The experimental results revealed that the proposed model could approximate the equivalent electrical resistance of the conductive float stitches in knitted fabrics to an acceptable degree.

## Keywords

Float stitch, resistive network, geometric model, conductive knitted fabric

In recent years, conductive yarns have been widely employed in the textile industry for the production of a new generation of functional textiles, namely, smart textiles or so-called electronic textiles [1-3]. When conductive yarns are introduced into fabrics[4], traditional textile products are endowed with innovative functions with applications in fields such as health care[5], medicine[6], sports or outdoor activities[7][8], electromagnetic shielding[9][10], thermal product development [11-13], etc. Three approaches (knitting, weaving, and embroidering) are normally used to form conductive fabrics [14] [15]. Knitting is considered to be the most superior among these three approaches due to the resulting good elasticity and shape formation flexibility. To date, the most common knitting methods for embedding conductive yarns into fabrics are generally plain knitting, plating knitting, and intarsia knitting. However, these methods cannot meet all the electronic property requirements for conductive fabrics, such as adjustable resistance with limited fabric dimensions and density.

In the study of conductive fabrics, it was found that, besides transforming conductive yarns [16], variations in the knitted structures can change their electronic characteristics, and a few studies have been performed using different knitted stitch structures. In 2005, a wearable health care system called WEALTHY was developed by employing the intarsia tubular technique, which enabled the conductive yarn to appear on technical back of a double-faced fabric, thus insulating the conductive yarn from the outside environment [17]. However, this system cannot overcome the limitation of resistance requirements, i.e. it cannot deal with variable resistance of knitted fabrics within a definite area. In another example, Liu introduced some structures that were not limited to plain knitting, including 2x1 rib, miss-knit, and mesh structure [18]. But, these structures were only employed as the non-conductive parts, while the conductive parts still used the simple plating knitting technique. These deficiencies appear to have recently come to the attention of researchers. In the novel design of intelligent clothing developed by Li et al., a full Milano stitch, 2x2 rib stitch, and tubular stitch were introduced [19-24]. A knitted stretch sensor used as a

breathing rate indicator was developed by Waqas et al., [25] in the research of which four ordinary knitted structures (plain jersey, 1x1 rib, interlock, and floating) were tested and compared to select the most suitable structure for monitoring breathing. A few complex knitted structures, such as the cross-miss 1x1 plain knitted structure, lacoste, interlock, and double pique, were employed in the study of the electromagnetic shielding properties of conductive knitted fabrics by Ceken et al. [9][26]. Nevertheless, the lack of a theoretical analysis in the geometric structure of knitted fabrics is a common problem existed in the previous studies. In an investigation conducted by the University of Manchester examining the thermo-mechanical behaviour of a knitted heating fabric, three different structures (plain jersey, rib, and interlock) were analysed from the viewpoint of their knitted loop geometry. However, the contact resistance (generated by interlap of two conductive yarns), which together with the linear resistance (proportional to length of conductive yarns) that contributes to the overall resistance of the conductive knitted fabric, was not mentioned in the study [27]. Some research introduced matrix expression to obtain the resistance value of single jersey [28] and 1x1 rib [29] on the base of a loop model. It was found that contact resistance  $R_c$  was proposed to denote the resistance of overlap of two neighbour loops in wales direction. Based on the division of the resistance of the knitted loop into the linear and contact resistances, Li's group [30] performed a theoretical analysis of the resistive effects of plain jersey conductive knitted stitches and proposed a resistive network model for predicting the electrical resistance of a conductive knitted fabric. A hexagonal model was proposed to represent plain weft knitted structure in Wang et al.'s [31][32] study where the resistance variation of elastic knitted conductive fabric under biaxial strain was investigated from theoretical study to experimental verification.

It is well known that the knit, tuck, and float are the three basic elements in the formation of knitted fabrics, and plain jersey fabric is only composed of knit stitches. Therefore, the tuck and float stitches are two other very significant factors for further research on the electrical properties of conductive fabrics. The study of the tuck stitch can be conducted on the basis of the float stitch; thus, in this study, the resistive impact of float stitches on conductive knitted fabrics was a priority. A geometric model was built to accurately represent the knitted loop stitches in the Cartesian coordinate system. Then, a model of float stitches was established on the basis of this

geometric model to enable the evaluation of the equivalent electrical resistance in different parts of conductive knitted fabrics with float stitches. A resistive network model for conductive fabrics with different numbers of courses and wales was derived. A series of corresponding experiments were conducted. The results of the comparison between the modelled and measured electrical resistances of the conductive knitted fabrics with float stitches were discussed. This study showed that the geometric model incorporated with the resistive network could effectively approximate the electrical resistance with an acceptable error range. Future work will be performed to improve the accuracy and efficiency of the proposed model. The derived model could provide additional insight into the physical properties of conductive knitted fabrics with conductive float stitches, establish basic principles for the design and feasible manipulation of conductive knitted garments, and enable diversification of the existing knitting methods for embedding conductive yarns in knitted structures.

## **The experimental design**

### ***Equipment and material***

All samples were manufactured on an E7.2 STOLL CMS 822 computerised flat knitting machine because of the powerful pattern design functionality. In the experiments, the samples were knitted with normal and conductive yarn. The normal yarn was 100% merino wool, and its count was 30/2 Nm; the conductive yarn was made from Nylon 66 fibers coated with silver, the resistance of which was 1  $\Omega/\text{cm}$ , and its count was 47 Tex. The standard deviation of the conductive yarn's resistance is 0.02.

## Structure selection

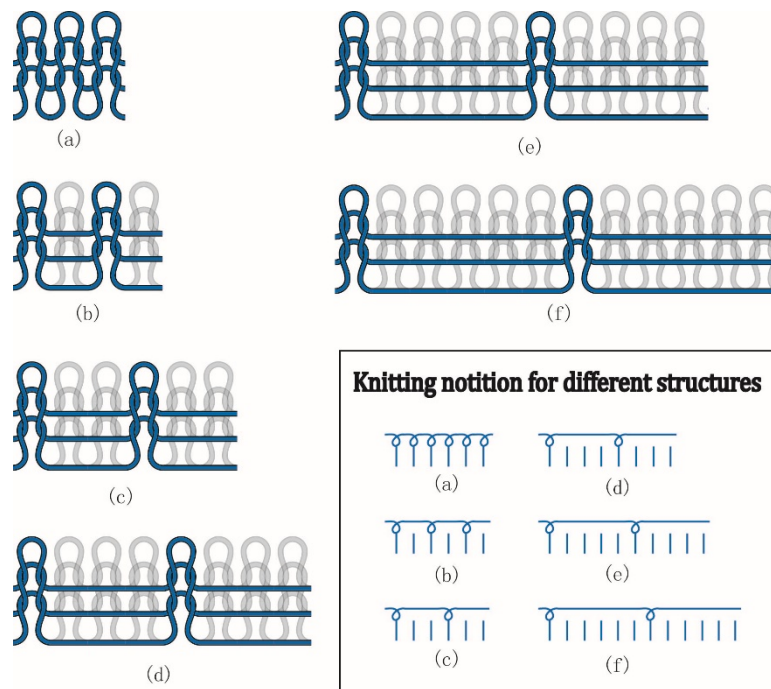


**Figure 1.** (a) plain weft knitted fabric; (b) 1x1 float; (c) 1x2 float; (d) 1x3 float; (e) 1x4 float; (f) 1x5 float.

The float structure was developed by one knitted loop stitch followed by a fixed number of float stitches. For example, the 1xn float structure was composed of one integrated knit loop stitch and n float stitches. Additionally, the plain weft knitted structure was knitted to serve as the reference. Six different structures, including the plain weft knitted structure and 1x1, 1x2, 1x3, 1x4, and 1x5 floats, were manufactured as shown in Figure 1.

## Sample preparation

For STOLL(H. Stoll GmbH & Co. KG) computerized flat knitting machine, fabrics' density was mainly controlled by NP value which is a machine parameter to adjust needle's downwards position of loop formation. In the experiment, NP value was adjusted to 12.0 which is a normal value for single face fabric on flat knitting machine. As a result, the density of all the samples was 8.62 courses per cm and 7.14 wales per cm in wales and course direction respectively. The fabric was uniform, with a dimension of 100 courses x 100 wales, and multi-layer knitting technology was employed. For the aim of dimensional stability, the conductive area was knitted with

two layers which were constituted by one conductive layer with float structures and the other one non-conductive layer with the back jersey structure. As shown in Figure

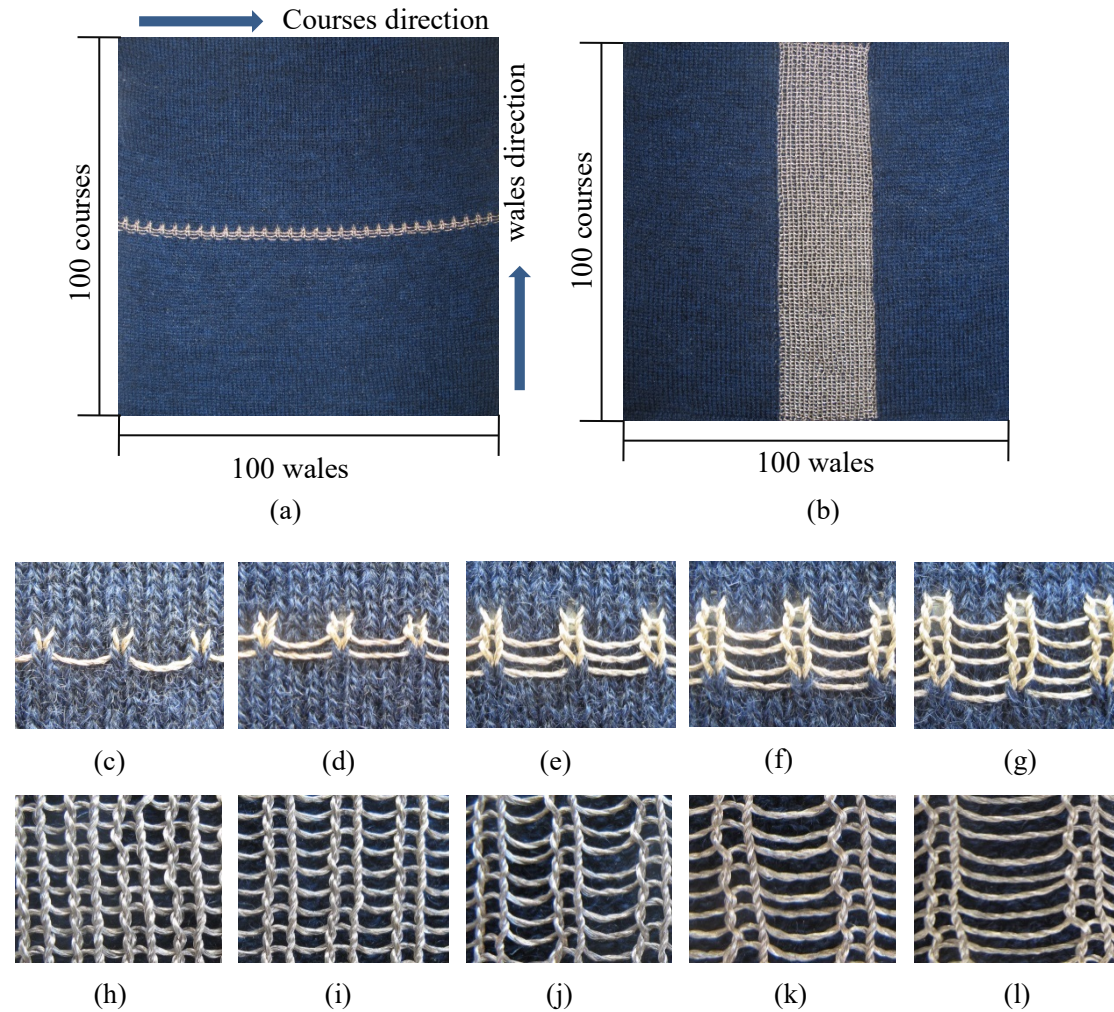


**Figure 2.** Sample pieces of (a) Series 1; (b) Series 2; In series 1, partial images of structure 1x3 float knitted with (c) one course; (d) two courses; (e) three courses; (f) four courses; (g) five courses; In series 2, partial images of structure (h) 1x1 float; (i) 1x2 float; (j) 1x3 float; (k) 1x4 float; (l) 1x5 float.

2 (a) and (b), the samples were knitted in two series, with the conductive yarn distributed in the courses and wales directions, and three identical swatches of each design were prepared to strengthen the results. Due to the different influences of the float stitches in the courses and wales directions, series 1 was designed to determine the relationship between the resistance and the different float structures with variable course numbers, and series 2 was designed to determine the relationship between the resistance and variable float length in the float structures. Therefore, in series 1, the samples were prepared by knitting the conductive yarn fixed within 100 wales for six

different structures, and the number of courses was varied from 1 to 5. Figure 2 (c) to (g) shows the fabric images for 1x3 float structure knitted with one course to five courses. To effectively investigate the influence of the float stitch with a varied number of wales, samples with too few repeat pattern units were not considered in our study. Therefore, in series 2, the samples were prepared by knitting the conductive yarn using 100 fixed courses in six different structures, and 10 horizontal repeat pattern units were included in every structure, i.e., the number of wales was varied to be 10 courses for the jersey, 20 courses for the 1x1 float, 30 courses for the 1x2 float, 40 courses for the 1x3 float, 50 courses for the 1x4 float, and 60 courses for the 1x5 float structures. Figure 2 (h) to (l) illustrates the fabric images of series 2 knitted with 1x1 float, 1x2 float, 1x3 float, 1x4 float and 1x5 float structures, respectively. After leaving the machine, the samples were laid out on a platform for 24 hours without ironing or laundering.

## **The theoretical model**

### ***The establishment of a float structure model***

To date, mathematical models for knitted fabrics have been proposed based on planar and spatial spaces, including purely geometric models, mechanical models, and models for pressure and heat-moisture transmission prediction [33]. In our research, the knitted fabric is assumed to be in a fully relaxed state, i.e., a configuration of minimum energy; therefore, a 2D geometric model was established to describe the knitted stitches. Previously, many researchers have proposed their geometrical models, for example, Pirece [34], Leaf and Glaskin [35], Munden [36], Postle [37] and Semnani et al. [38]. Munden's model is one of the classical models illustrate the relationship between the length of yarn and the dimension of the knitted loop in plain knitted fabrics [36]. The fundamental principle is that the dimension of a loop in a knitted fabric is transformable and depends on its loop length; however, the shape of a knitted loop is assumed to be fixed, i.e., every part of a knitted loop is always proportional to its loop length, which is shown in figure 3. In figure 3, loop 2 is proportional to loop 1 and the expression  $\frac{OA}{OA_1} = \frac{OB}{OB_1} = \frac{OC}{OC_1} = p$  is established, where  $p$  is the ratio of the lengths of loops 1 and 2.

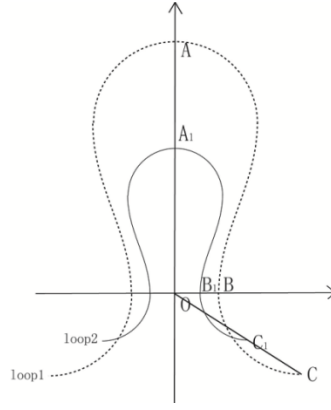


**Figure 3.** The two similar loops in Munden's geometric model.

Therefore, based on Munden's model, a geometric model can be established by representing the loop pillar as a sine function and the loop arc as a semi-circular function. Figure 4(a) is the established loop geometric model for a single yarn of negligible diameter in a Cartesian coordinate system, and Figure 4(b) represents a case in which the diameter cannot be ignored. The midpoint of the shortest straight line drawn within the loop (line E'E) is defined as the original point.

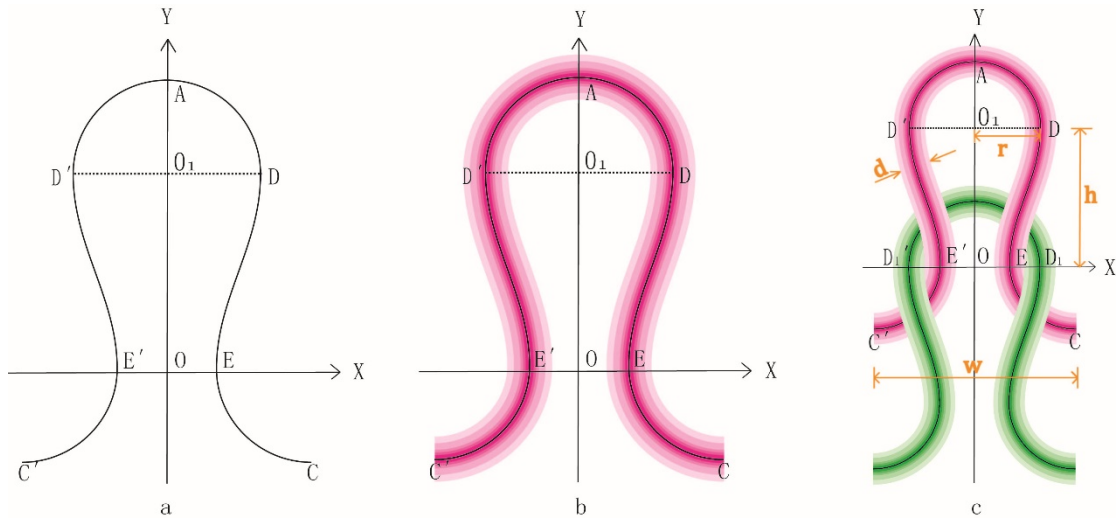


**Figure 4.** (a) The geometric model displayed by the axis line of the yarn; (b) The geometric model displayed by yarn with a certain diameter; (c) Two adjacent loops in wales direction interlocked each other.

Figure 4(c) demonstrates the interlocked form of two adjacent loops in wales direction, from which it is observed that the sinker loop of the upper loop (in pink color) connects to the needle loop of the lower loop (in green color) tightly. Therefore, it is



proposed that the distance of  $D_1'E'$  is equal to yarn's diameter in the geometrical model. For curve  $E'D'$ ,  $x$  can be recognized as a sine function in which the amplitude is half of  $D_1'E'$ , the period is twice of  $OO_1$  and phase shift is  $(-O_1D' + \frac{D_1'E'}{2}, \frac{OO_1}{2})$ . For easy expression, definitions are given out as shown in figure 4(c):  $r$  is the radius of semi-circle  $D'AD$ ,  $d$  is the diameter of the knitted yarn,  $w$  is the distance between two adjacent stitches in the wales direction (wales distance), and  $h$  is the distance between two adjacent stitches in the course direction (courses distance). Therefore, equation (1) is established to describe the relational expression between  $x$  and  $y$  for curve  $E'D'$ .

$$-x = \frac{d}{2} \sin \left( \frac{\pi}{h} y - \frac{h}{2} \right) - \left[ - \left( r - \frac{d}{2} \right) \right] \quad (1)$$

In the same way, the relational expression between  $x$  and  $y$  for curve  $DE$  can be obtained as well.

As a result, the loop can be expressed with the following set of equations (2) to (6):

$$y_1 = -\sqrt{r^2 - (x_1 + \frac{w}{2})^2} \quad \left( -\frac{w}{2} \leq x_1 \leq -\frac{w}{2} + r \right) \quad \widehat{C'E'} \quad (2)$$

$$y_2 = \frac{h}{\pi} \sin^{-1} \left[ 1 - \frac{2(x_2 + r)}{d} \right] + \frac{h}{2} \quad \left( -r \leq x_2 \leq -\frac{w}{2} + r \right) \quad \widehat{E'D'} \quad (3)$$

$$y_3 = \sqrt{r^2 - x_3^2} + h \quad \left( -r \leq x_3 \leq r \right) \quad \widehat{D'AD} \quad (4)$$

$$y_4 = \frac{h}{\pi} \sin^{-1} \left[ 1 - \frac{2(r - x_4)}{d} \right] + \frac{h}{2} \quad \left( \frac{w}{2} - r \leq x_4 \leq r \right) \quad \widehat{DE} \quad (5)$$

$$y_5 = -\sqrt{r^2 - (x_5 - \frac{w}{2})^2} \quad \left( \frac{w}{2} - r \leq x_5 \leq \frac{w}{2} \right) \quad \widehat{EC} \quad (6)$$

where  $x_1$  and  $y_1$  are  $x$  and  $y$  coordinate values for curve  $C'E'$  in the Cartesian coordinate system; and in the same way,  $x_2$  and  $y_2$  are for curve  $E'D'$ ,  $x_3$  and  $y_3$  are for curve  $D'AD$ ,  $x_4$  and  $y_4$  are for curve  $DE$ ,  $x_5$  and  $y_5$  are for curve  $EC$ , respectively.

The model fit for float stitches can be established by treating the float yarn as an

extended line paralleled to the x-axis, as shown in Figure 5.

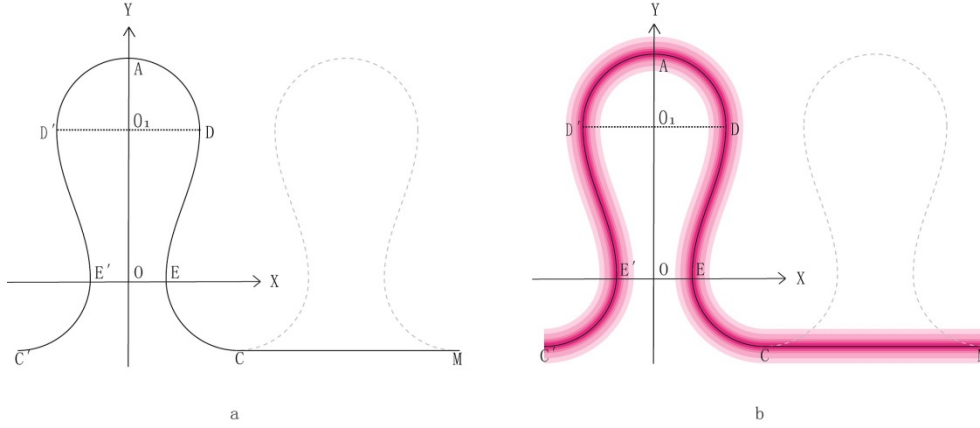


**Figure 5.** (a) The geometric model of a float knitted structure displayed by the axis line of the yarn; (b) The geometric model of a float knitted structure displayed by yarn with a certain diameter.

In Figure 5, the straight-line CM parallels to the x-axis represents the float yarn in a float knitted structure, and the length of CM is  $n$  times the wales distance ( $n$  is the number of float stitches in a repeatable pattern area determined by the structure of the knitted fabric required). Therefore, CM can be expressed by equation (7) as below:

$$y_6 = -r \quad \left( \frac{w}{2} \leq x_6 \leq \left( \frac{1}{2} + n \right) w \right) \quad (7)$$

Generally there is a slightly shape discrepancy between loops knitted with different yarns, however, the same models for the same structures with conductive yarns and non-conductive yarns are adopted in this paper because the research purpose does not focus on it.

### Resistive representation for different parts of the model

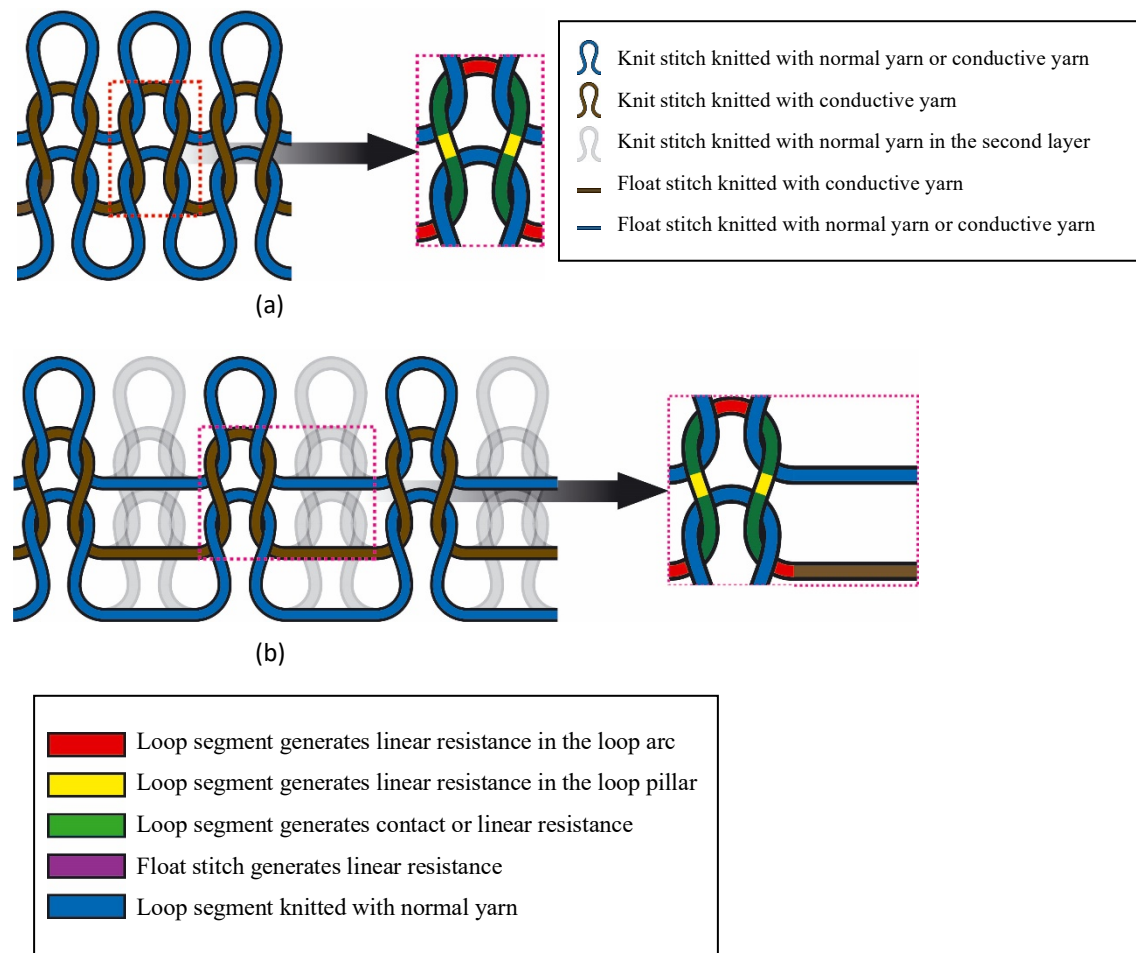


**Figure 6.** (a) Interlocked state of a pattern unit in a plain knitted structure; (b) Interlocked state of a pattern unit in a float knitted structure.



When a single loop is interlocked with two neighbouring loops in the upper and lower sides, it can be divided into nine sections, which are distinguished by different colours in Figure 6(a). In these nine sections, the red parts are the linear resistances in the loop arc; the yellow parts are the linear resistances in the loop pillar; and the green parts can generate contact resistance when the upper or lower loop is knitted with conductive yarn, otherwise, the green parts represent the linear resistance in the loop pillar and arc.

In float knitted structures, in addition to the nine different sections in plain knitted structures, there is a linear resistance of the float stitches coloured purple in Figure 6(b). It has been observed that a plain knitted structure and a float knitted structure can be distinguished based on whether a float yarn exists in the knitted fabric. For a

1xn float structure, when  $n=0$ , the knitted structure is simply the plain knitted structure. Therefore, the model of a plain knitted structure is included in the model of a float knitted structure in the case where  $n=0$ , as shown below. As a consequence, the four different resistive networks associated with one pattern unit are listed in Table 1.

**Table 1.** Resistive network of one pattern unit in four different situations.

Option	Upper loop	Lower loop	Resistive work
1)	Knitted without conductive yarn	Knitted without conductive yarn	
2)	Knitted without conductive yarn	Knitted with conductive yarn	
3)	Knitted with conductive yarn	Knitted without conductive yarn	
4)	Knitted with conductive yarn	Knitted with conductive yarn	

In Table 1, the grey colour icon  represents contact resistance and the blue colour icon  represents linear resistance.  $R_H$  is the linear resistance in the loop arc between two loop pillars (red parts);  $R_V$  is the linear resistance in the loop pillar (yellow parts);  $R_C$  is the contact resistance between the linear resistance  $R_H$  and  $R_V$  (green parts);  $R_N$  is the linear resistance between the linear resistance  $R_H$  and  $R_V$  (green parts); and  $R_F$  is the linear resistance generated by one float stitch.

## *Resistive network model for different distributions of conductive yarn in knitted fabrics*

### *In case of distribution in the courses direction*

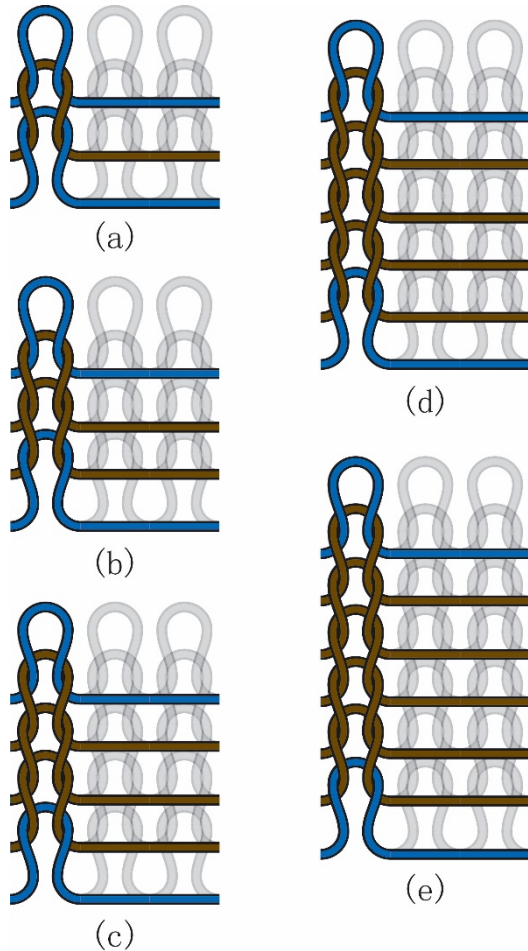


**Figure 7.**

- (a) Conductive yarn knits in one course;
- (b) Conductive yarn knits in two courses;
- (c) Conductive yarn knits in three courses;
- (d) Conductive yarn knits in four courses;
- (e) Conductive yarn knits five courses.

Conductive yarn may be knitted into fabric with different arrangements of wales and courses. For convenience,  $k$  is defined as the number of conductive knitting wales, and  $j$  is defined as the number of conductive knitting courses. In the sections below, the resistive network of the conductive knitted stitches for different numbers of courses is introduced. Figure 7 illustrates the interlocked status of the conductive yarn with normal yarn when it was knitted into fabric with one to five courses. It was observed that: 1) there was no contact resistance if only one course was knitted with conductive yarn; 2) contact resistance needed to be considered when two successive courses were knitted with conductive yarns, as there was an area in overlap between two adjacent loops in the wales direction; and 3) in case of three or more conductive knitted courses, a repeatable area was derived between the first and last course. The

corresponding resistive network may be drawn as follows:

*Conductive yarn knits, one course (j=1).*

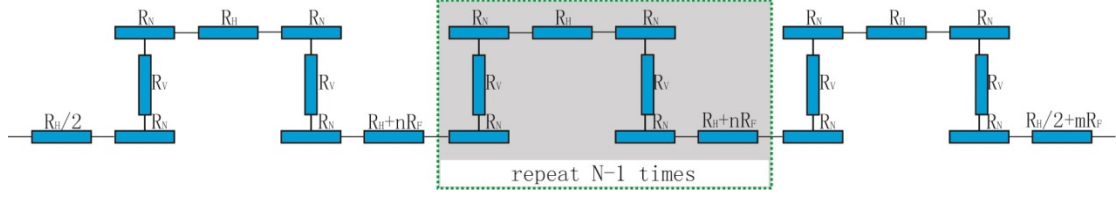


**Figure 8.** The resistive network for one course of conductive yarn knits

In Figure 8, the resistive network outlined by the green square and shaded in grey is a repeating area in the course direction.  $N$  is the number of integrated repeating pattern units, i.e.,  $N$  is the integer part of the result of the wales number ( $k$ ) divided by  $n+1$ , and  $m$  (the float stitch number following with the last knitted loop stitch in a course) can be calculated by equation (8):

$$m = k - N(n + 1) - 1 \quad (8)$$

Therefore, the resistive value can be represented by equation (9):

$$R = (N + 1)(R_H + 2R_V + 4R_N) + (k - N - 1)R_F \quad (9)$$

*Conductive yarn knits with two continuous courses (j=2).*

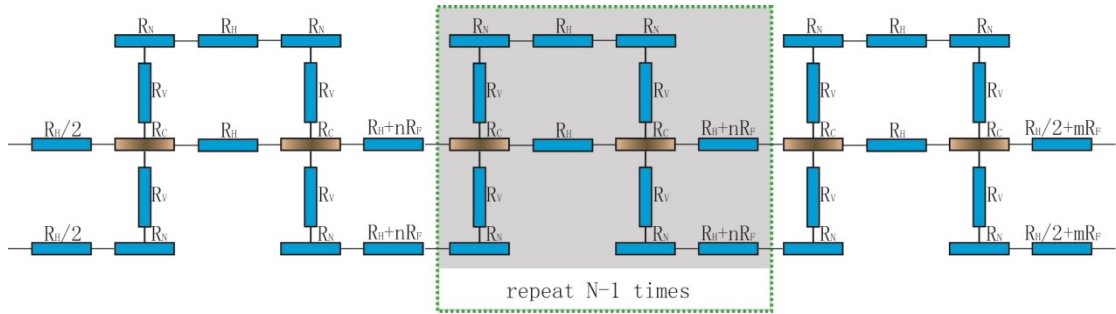


**Figure 9.** The resistive network when  $j=2$ .

Figure 9 shows the resistive network of conductive knitted stitches with two courses, and the area enclosed by the green square and shaded in grey is the repeating area in the horizontal direction, as in Figure 8. As discussed above, the contact resistance  $R_C$

generated in this situation is connected by four linear resistances in four directions. The computation of the resistance for the resistive network in this case is quite complex. For simplicity, Li et al. [30] treated the contact resistance  $R_C$  in the crossover of the two wires as four quarters of the  $R_C$  distributed to its four neighbouring branches, as shown in Figure 10 below.

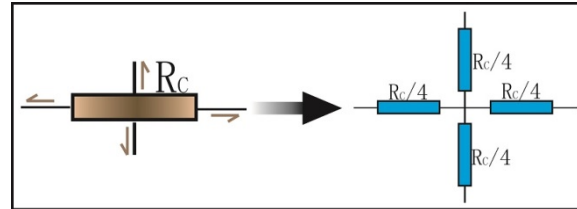


**Figure 10.** The treatment of crossover resistance.

By inserting the modified  $R_C$  into the original resistive network, the resistive network is converted to a network without crossover resistances (Figure 11).

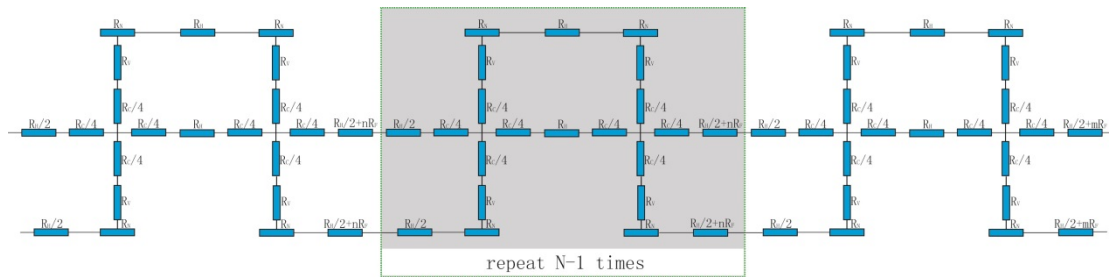


**Figure 11.** The converted resistance network when  $j=2$ .

In Figure 11, edge resistances may be ignored because they have little influence on the entire network when  $N$  is sufficiently large; thus, the resistive network can be further simplified.

To calculate the above resistive network, four combined resistance symbols, namely  $R_1$ ,  $R_2$ ,  $R_3$ , and  $R_4$ , are used throughout this paper, and they can be calculated by equations (10) to (13).  $R_1$  and  $R_3$  may be regarded as the inner resistances generated in the knit and float stitches, respectively.  $R_2$  and  $R_4$  may be regarded as the outer resistances, which are located in the boundary parts of the knit and float stitches and are connected to the non-conductive area, respectively.

$$R_1 = R_H + 0.5R_C \quad (10)$$

$$R_2 = R_H + 2R_N + 2R_V + 0.5R_C \quad (11)$$

$$R_3 = R_H + nR_F + 0.5R_C \quad (12)$$

$$R_4 = 2R_V + 2R_N + R_H + nR_F + 0.5R_C \quad (13)$$

By importing  $R_1$ ,  $R_2$ ,  $R_3$ , and  $R_4$ , the resistive network in Figure 10 becomes simplified, as shown in Figure 12.

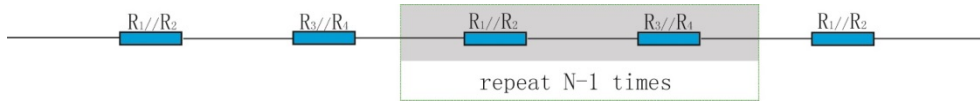


**Figure 12.** The simplified resistive network when  $j=2$ .

According to Figure 12, the resistance of the overall resistive network can be expressed by equation (14).

$$R = \frac{R_1 R_2}{R_1 + R_2} (N + 1) + \frac{R_3 R_4}{R_3 + R_4} N \quad (14)$$

*Conductive yarn knits with three or more courses ( $k \geq 3$ ).*

If the conductive yarn knits three or more courses, the repeating area will not only appear in the horizontal but also in the vertical direction. The original resistive network is shown in Figure 13.

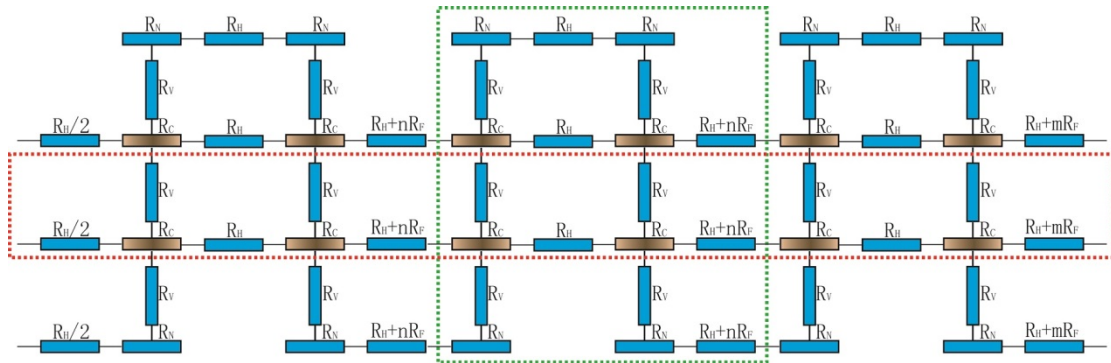


**Figure 13.** The original resistive network when  $j \geq 3$ .



In Figure 13, the resistive network enclosed by the green dashed square is the repeated area in the horizontal direction; the resistive network in red is the repeated area in the vertical direction. Similarly, the crossover contact resistance  $R_C$  is transferred to its four neighbouring lines, and the original resistive network is transformed to a resistive network without crossover resistances, as shown in Figure 14:

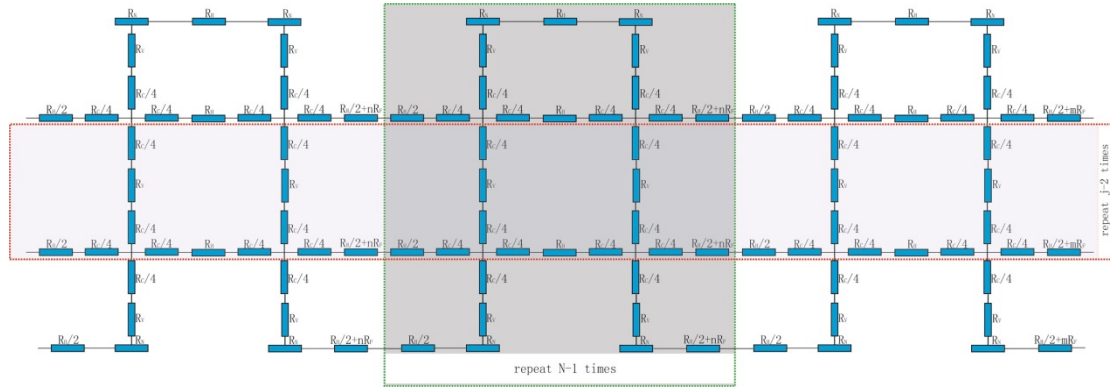


**Figure 14.** The resistive network after transformation when  $j \geq 3$ .

The resistances at the edge are ignored again; then, by introducing equations (10) to (13) and using equation (15) for  $R_5$  to replace the resistors in the vertical direction between the blocks, the resistive network is simplified as shown in Figure 15.

$$R_5 = R_V + 0.5R_C \quad (15)$$

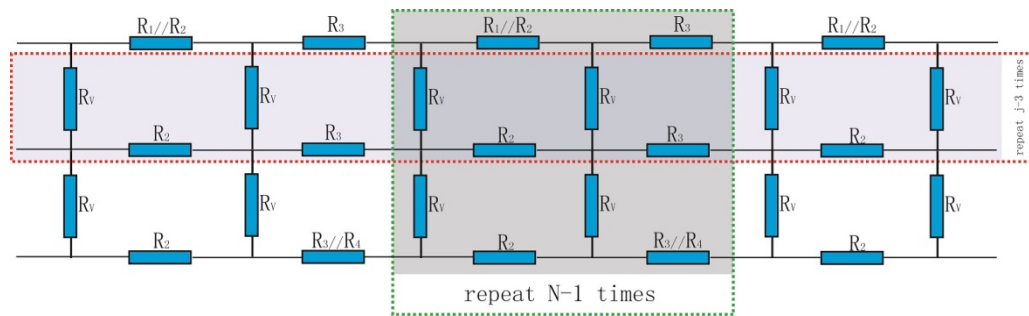


**Figure 15.** The simplified resistive network when  $j \geq 3$ .

Computation of the resulting resistive network based on the resistances that exist in both the horizontal and vertical routes is now too complicated to solve. However, the resistances in the vertical routes may be eliminated by applying the signal flow graph

theory [39]. Two additional resistances,  $\Delta_1$  and  $\Delta_2$ , are added to the resistive network to give the overall resistive network an equipotential distribution in the horizontal direction. Therefore, no current will flow in the vertical direction. The expressions of  $\Delta_1$  and  $\Delta_2$  are represented by equations (16) and (17).

$$\Delta_1 = \frac{R_2^2 R_3}{(R_1 + R_2)(R_2 + R_3)} \quad (16)$$

$$\Delta_2 = \frac{R_2^2 R_3}{(R_3 + R_4)(R_2 + R_3)} \quad (17)$$

According to the signal flow graph theory, the simplified resistive network is updated as shown in Figure 16.

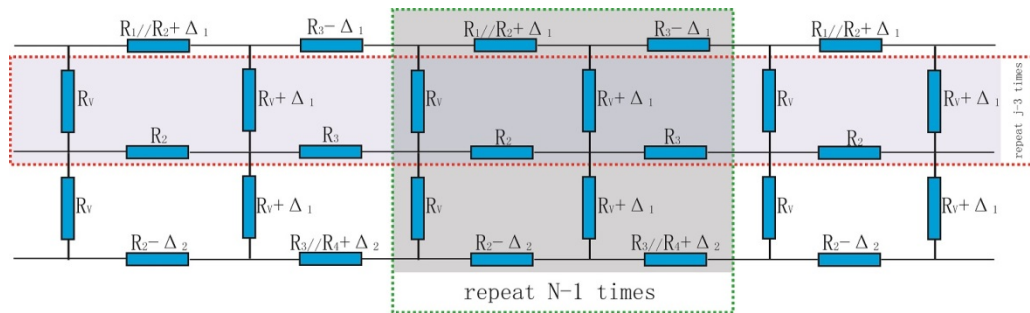


**Figure 16.** The equivalent resistance when  $j \geq 3$  after applying signal flow graph theory.

In principle,  $\Delta_1$  and  $\Delta_2$  are introduced to make the ratio of the two adjacent resistances in the horizontal route equal. In Figure 16, because

$$\frac{R_1 \parallel R_2 + \Delta_1}{R_3 - \Delta_1} = \frac{R_2}{R_3} = \frac{R_2 - \Delta_2}{R_3 \parallel R_4 + \Delta_2},$$

resistors in the vertical routes can be eliminated as illustrated in Figure 17.

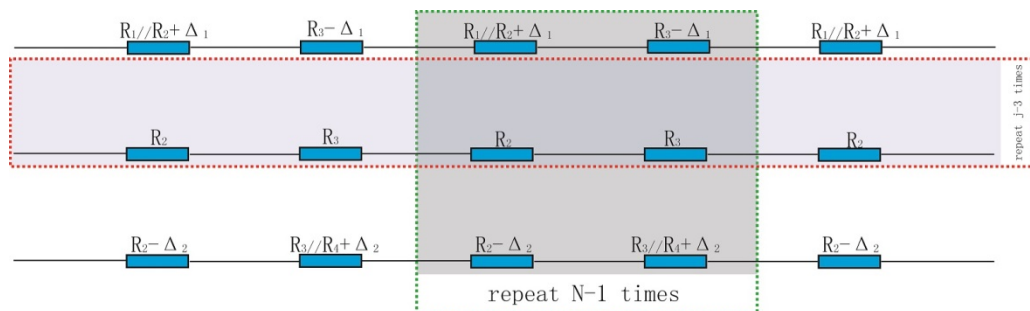


**Figure 17.** The equivalent resistance when  $j \geq 3$  after eliminating the vertical resistors.

After eliminating the vertical resistors, the resistance of the float knitted structure  $1 \times n$  with a certain wales number  $k$  and course number  $j$  is computable and expressed by equation group (18). The resistors  $R_1$ ,  $R_2$ ,  $R_3$ , and  $R_4$  are again defined by the previous equations (10) to (13), and the resistors  $R_A$ ,  $R_B$ , and  $R_C$  are defined by equations (19) to (21).

$$\left\{ \begin{array}{ll} (N + 1)(R_H + 2R_V + 4R_N) + (100 - N - 1)R_F & j = 1 \\ \frac{R_1 R_2}{R_1 + R_2} (N + 1) + \frac{R_3 R_4}{R_3 + R_4} N & j = 2 \\ \frac{1}{\frac{1}{R_A} + \frac{(k-3)}{R_B} + \frac{1}{R_C}} & j \geq 3 \end{array} \right. \quad (18)$$

$$R_A = N(R_1 \parallel R_2 + R_3)R_1 \parallel R_2 \quad (19)$$

$$R_B = N(R_2 + R_3) + R_2 \quad (20)$$

$$R_C = N(R_3 \parallel R_4 + R_2) + R_2 \quad (21)$$

*In the case of distribution in the wales direction*

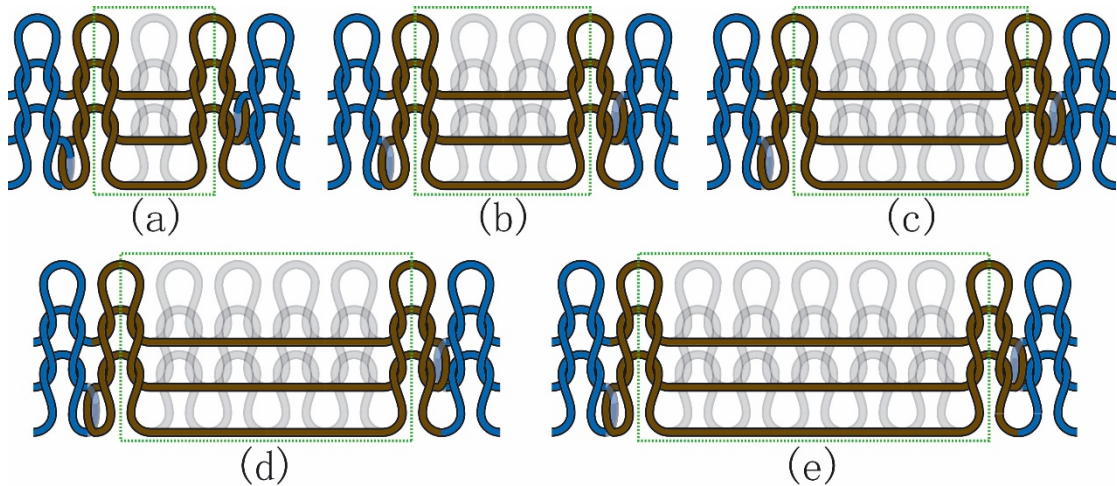


**Figure 18.** Float knitted stitches distributed in the horizontal direction of a knitted fabric: (a) 1x1 float, (b) 1x2 float, (c) 1x3 float, (d) 1x4 float, and (e) 1x5 float.

Float knitted structures can be designed as illustrated in Figure 18, and the pattern unit

(framed by green square) repeats partially in the horizontal direction and extends from top to bottom in fabrics to form a vertical distribution. Because there is no additional contact resistance accompanying the increase in the repeated unit in the course direction, Figure 13 can be utilised to illustrate the corresponding resistive network when  $k \geq 1$ . If the edge resistances are ignored again, the resistive network is equivalent to that shown in Figure 19.

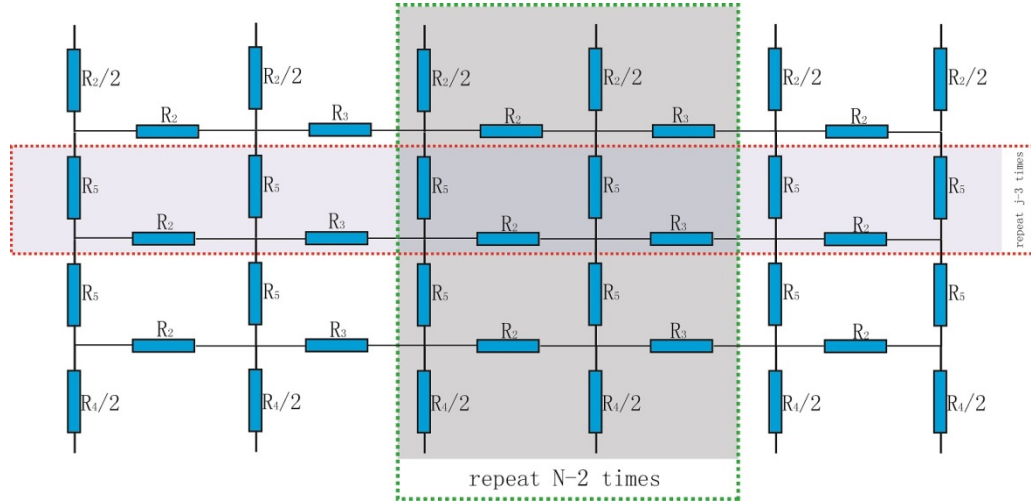


**Figure 19.** The equivalent resistive network for a wales distribution when  $k \geq 1$ .

Similarly, because the knitted structure is mainly symmetric, the resistors in the vertical direction in the network form an equipotential state in every block. There is negligible current flow through the horizontal resistors  $R_2$  and  $R_3$ . As a consequence, the horizontal resistors  $R_2$  and  $R_3$  may be eliminated, which will simplify the resistive network (Figure 20), and the corresponding resistance of the simplified resistance can be expressed by equation (22).

$$R = \frac{\frac{R_2}{2} + (j-2)R_5 + \frac{R_4}{2}}{N} \quad (k \geq 1) \quad (22)$$

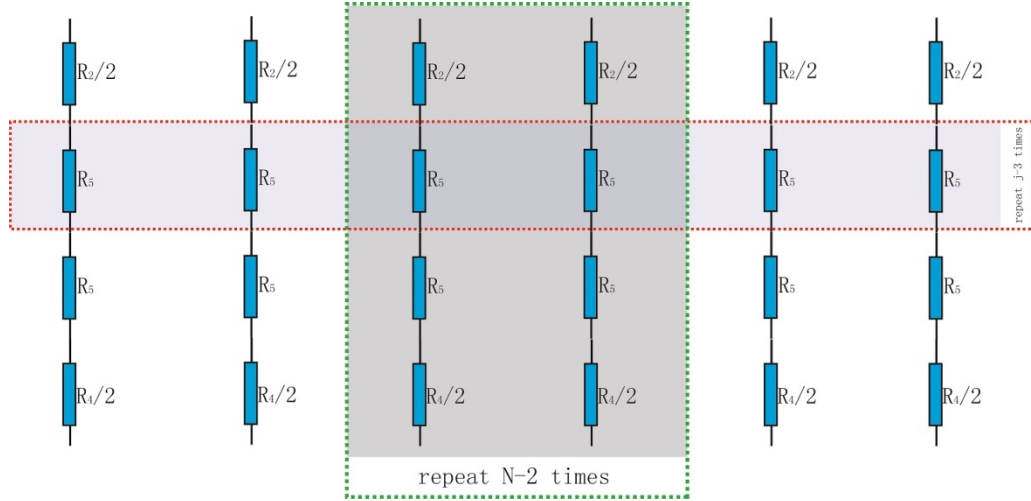


**Figure 20.** The final resistive network for the wales distribution when  $k \geq 1$ .

## Experimental results and discussion

### *The measurement of resistance values of knitted fabrics*

The resistances were measured using a 6 1/2 Digit 34401A Multimeter (Agilent Technologies, Palo Alto, CA). The testing points on the fabric samples for series 1 and 2 between which the resistance has been measured were illustrated in Figure 21 (a) and (b), respectively. The resistance values measured for series 1 and 2 are listed in Tables 2 and 3, respectively. The average measured values with error bars and simulated values are shown in Figures 23 and 24, respectively.

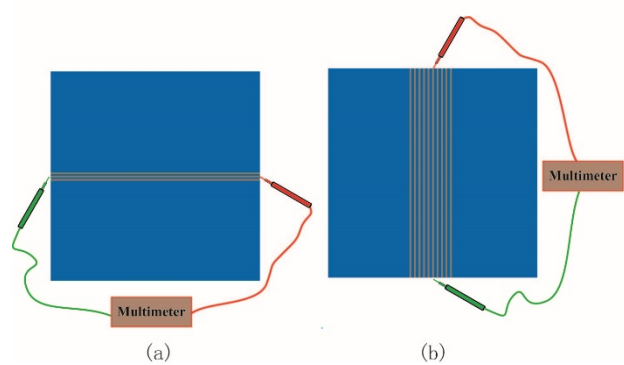


**Figure 21.** The testing illustration for measuring resistances by Multimeater in case of (a) series1; (b) series 2.

**Table 2.** The resistance values of different conductive fabrics with 100 wales and variable course numbers (Unit:  $\Omega$ ).

structure	jersey			float 1x1			float 1x2			float 1x3			float 1x4			float 1x5		
sample Code	S1	S2	S3	S1	S2	S3	S1	S2	S3	S1	S2	S3	S1	S2	S3	S1	S2	S3
course 1	78.9	79.7	79.7	50.4	51.3	51.0	38.2	40.4	39.9	36.3	36.1	37	33.8	32.5	32.8	28.5	29.8	29.7
course 2	34.9	35.5	35.1	22.4	22.8	23.1	18.5	18.2	18.1	15.9	16	16.2	14.8	15.5	15.1	13.9	14.2	14.0
course 3	22.2	22.0	22.7	13.9	13.6	13.4	11.3	11.2	11.3	9.8	9.6	10.0	9.0	9.3	9.2	8.8	8.7	8.6
course 4	15.2	15.3	16.0	10.0	10.7	10.5	8.6	8.7	9.3	8.1	7.7	8.2	7.2	6.9	7.1	6.6	6.3	6.7
course 5	12.8	12.4	12.9	7.9	7.8	8.0	6.9	7.9	7.1	6.2	6.3	6.3	5.5	5.4	5.8	5.3	5.4	5.5

**Table 3.** The resistive values of different conductive fabrics with 100 courses and variable course numbers (Unit:  $\Omega$ ).

structure	jersey			float 1x1			float 1x2			float 1x3			float 1x4			float 1x5		
Sample Code	S1	S2	S3	S1	S2	S3	S1	S2	S3	S1	S2	S3	S1	S2	S3	S1	S2	S3
course 10	1.62	1.63	1.61	-	-	-	-	-	-	-	-	-	-	-	-	-	-	-
course 20	-	-	-	1.67	1.71	1.58	-	-	-	-	-	-	-	-	-	-	-	-
course 30	-	-	-	-	-	-	1.67	1.83	1.72	-	-	-	-	-	-	-	-	-
course 40	-	-	-	-	-	-	-	-	-	1.79	1.75	1.82	-	-	-	-	-	-
course 50	-	-	-	-	-	-	-	-	-	-	-	-	1.79	1.77	1.82	-	-	-
course 60	-	-	-	-	-	-	-	-	-	-	-	-	-	-	-	1.77	1.82	1.86

### *The measurement of the loop model-related parameters $d$ , $w$ , $h$ , and $r$*

From the knitted swatches, the loop-related parameters  $d$ ,  $w$ , and  $h$  were measured. As shown in Table 4 each parameter was tested three times and the experimental data, as

well as their average value and standard deviation (SD), were also listed.

**Table 4.** Experimental values of the loop model-related parameters d, w, and h.

Parameter	Diameter of yarn(d)			Width of a loop (w)			Height of a loop (h)		
Times	1	2	3	1	2	3	1	2	3
Experimental Value(mm)	0.34	0.29	0.37	1.37	1.51	1.36	0.92	1.03	0.90
Mean(mm)	0.33			1.41			0.95		
Standard deviation	0.04041			0.08386			0.07		

According to the previous geometric model, r can be calculated as  $r = \frac{1}{4}(w + 2d)$ , which was approximately 0.52 mm.

#### ***The model equation group based on the experimental data***

By importing the experimental data from Table 4 into equation group (2) to (6), the updated equation group (23) to (27) was derived as follows:

$$y_1 = \sqrt{0.52^2 - (x_1 + \frac{1.41}{2})^2} \quad (-0.705 \leq x_1 \leq -0.185) \quad \widehat{C'E'} \quad (23)$$

$$y_2 = \frac{0.95}{\pi} \sin^{-1} \left[ 1 - \frac{2(x_2 + 0.52)}{0.33} \right] + \frac{0.95}{2} \quad (-0.52 \leq x_2 \leq -0.185) \quad \widehat{D'E'} \quad (24)$$

$$y_3 = \sqrt{0.52^2 - x_3^2} + 0.95 \quad (-0.52 \leq x_3 \leq -0.52) \quad \widehat{D'AD} \quad (25)$$

$$y_4 = \frac{0.95}{\pi} \sin^{-1} \left[ 1 - \frac{2(0.52 - x_4)}{d} \right] + \frac{0.95}{2} \quad (0.185 \leq x_4 \leq 0.52) \quad \widehat{DE} \quad (26)$$

$$y_5 = \sqrt{0.52^2 - (x_5 - \frac{1.41}{2})^2} \quad (0.185 \leq x_5 \leq 0.705) \quad \widehat{EC} \quad (27)$$

### The computation of intersection points *B* and *F*

The model of three loops interlocked one by one in the vertical direction is shown in Figure 22. In Figure 22, compared with loop **b**, loop **a** was considered to shift “*h*” on the *y* axis, and loop **c** was considered to shift “*-h*” on the *y* axis. The point of intersection *B* can be determined by equations (26) and (28):

$$y = \sqrt{0.52^2 - x^2} \quad (0 \leq x \leq 0.52) \quad \widehat{A_1D_1} \quad (28)$$

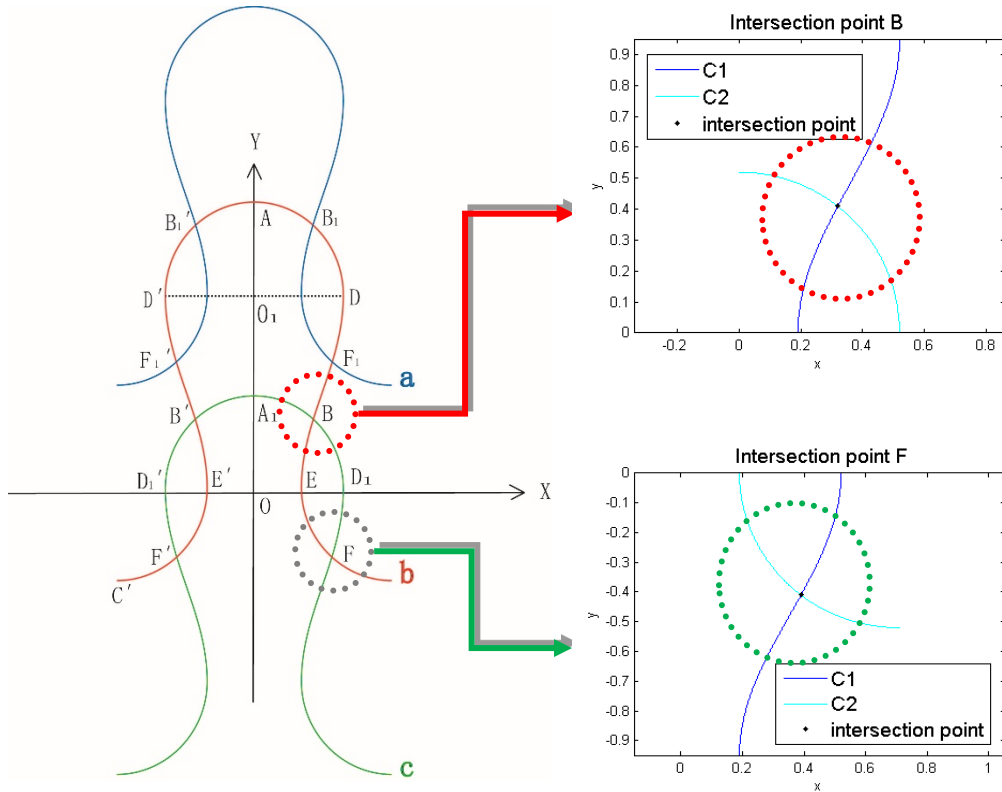


**Figure 22.** Three interlocking loops in the vertical direction.

By utilising MATLAB 2007a, point *B* ( $x_B$ ,  $y_B$ ) was calculated, and its *x* and *y* coordinate values were computed to be approximately 0.3198 and 0.4100, respectively. Similarly, another important intersection point, *F* ( $x_F$ ,  $y_F$ ), was calculated, and the *x* and *y* coordinate values were computed to be approximately 0.3902 and -0.4100, respectively.



### *The computation of the curve length*

A parametric equation (30) used to demonstrate the Curve  $\widehat{DE}$  was established on the basis of equation (29).

$$t = \frac{\pi}{0.95}y - \frac{\pi}{2} \quad (29)$$

$$\begin{cases} x = \frac{0.33}{2} \sin t + 0.52 - \frac{0.33}{2} \\ y = \frac{0.95}{\pi} t + \frac{0.95}{2} \end{cases} \quad (30)$$

According with the theory of Definite Integral, the length of a curve can be calculated by equation (31):

$$s = \int_a^b \sqrt{(\phi'(t))^2 + (\varphi'(t))^2} dt \quad (31)$$

Thus, the length of curve  $\widehat{BE}$  was computed by equation (32):

$$s_{BE} = \int_{-\frac{\pi}{2}}^{\frac{0.31980}{0.95} - \frac{\pi}{2}} \sqrt{\left(\frac{0.33}{2} \cos t\right)^2 + \left(\frac{0.95}{\pi}\right)^2} dt \quad (32)$$

The length of curve  $\widehat{BD}$  was computed by equation (33):

$$s_{BD} = \int_{\frac{0.31980}{0.95} - \frac{\pi}{2}}^{\frac{\pi}{2}} \sqrt{\left(\frac{0.33}{2} \cos t\right)^2 + \left(\frac{0.95}{\pi}\right)^2} dt \quad (33)$$

By utilising MATLAB 2007a, the approximate value of the curve length can be derived as:

$$s_{BE} = 0.3333 ; s_{BD} = 0.6836.$$

The curve  $\widehat{D_1F}$  can be defined as a definite integral by the following integral equation (34):

$$s_{D_1F} = \int_{-\frac{\pi}{2}}^{\frac{\pi}{2}} \sqrt{\left(\frac{0.33}{2} \cos t\right)^2 + \left(\frac{0.95}{\pi}\right)^2} dt \quad (34)$$

The curve  $\widehat{FE_1}$  can be defined as a definite integral by the following integral equation (35):

$$s_{FE_1} = \int_{-\frac{\pi}{2}}^{\frac{\pi}{2}} \sqrt{\left(\frac{0.33}{2} \cos t\right)^2 + \left(\frac{0.95}{\pi}\right)^2} dt \quad (35)$$

The approximate value of a curve length can be derived by MATLAB:

$$s_{D_1F} = 0.4347 ; s_{FE_1} = 0.5825.$$

Similarly, by inserting intersection point F (0.3902, -0.4100) into equation (26), the curve length can be defined as a definite integral with the following results:

$$s_{EF} = 0.4724; s_{FC} = 0.3444.$$

Due to the circular symmetry of curve  $\widehat{EC}$  and curve  $\widehat{AD}$ , it can be concluded that:

$$s_{B_1D} = 0.4724; s_{AB_1} = 0.3444.$$

Thus far, the curve lengths of the nine sections divided by the interlocking of the loops in an integrate loop can all be derived from the computed curve length and the experimental data. The linear resistances related to the curve lengths are displayed below:

$$s_{B_1'B_1} = 2s_{AB_1} = 0.6888\text{mm};$$

$$s_{BF_1} = s_{BD} - s_{D_1F} = 0.2468\text{mm};$$

$$s_{B_1F_1} = s_{B_1D} + s_{DF_1} = 0.9071\text{mm};$$

$$s_{CM} = w = 1.41\text{mm}.$$

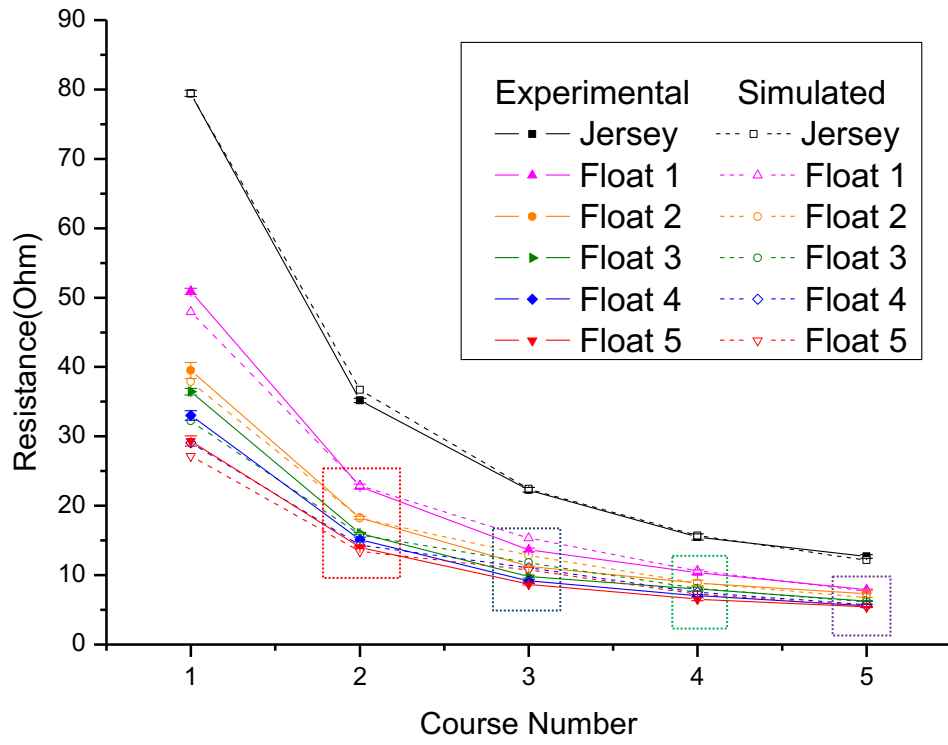
***The proportional relationship of the linear resistances  $R_H$ ,  $R_V$ ,  $R_N$ , and  $R_F$  based on the geometric loop model***

Because the linear resistance changes in proportion to the length of yarn, based on the above computation, the resistance values for  $R_H$ ,  $R_V$ ,  $R_N$ , and  $R_F$  can be deduced as below:

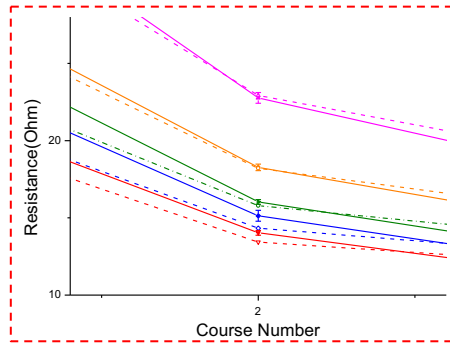
$$R_H = 0.06888\Omega; R_V = 0.02468\Omega; R_N = 0.09071\Omega; R_F = 0.141\Omega.$$

Therefore, the proportional relationship of the linear resistances  $R_H$ ,  $R_V$ ,  $R_N$ , and  $R_F$  was 0.6888: 0.2468: 0.9071: 1.410.

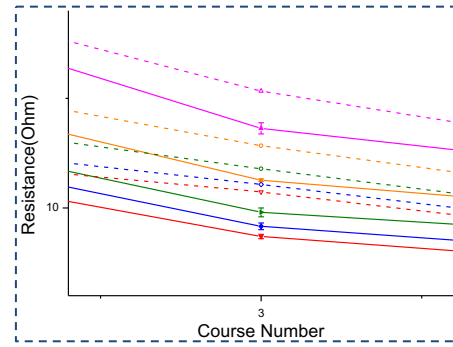
### The simulation results



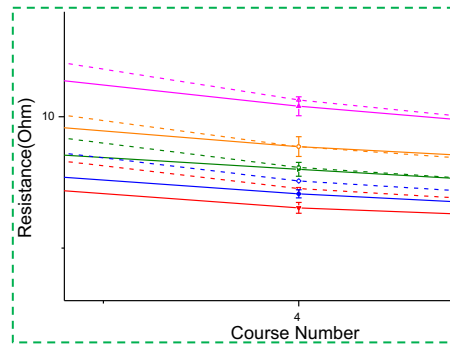
(a)



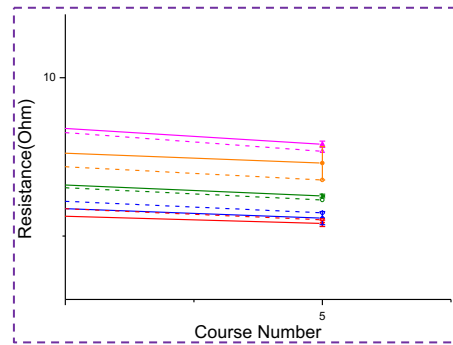
(b)



(c)



(d)



(e)

**Figure 23.** (a) The simulated and experimental resistance results for different structures with 100 fixed wales and variable course numbers; Enlarged area of the crowded sections framed by dashed rectangles in (b) red color; (c) blue color; (d) green color; (e) purple color.

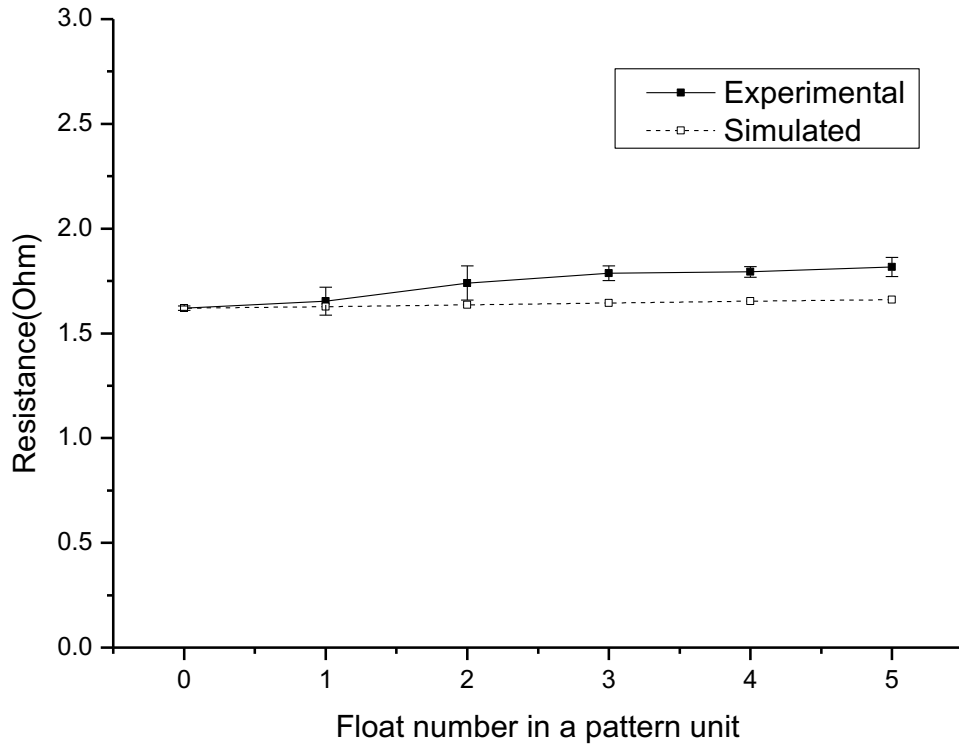


**Figure 24.** The simulated and experimental resistance results for different structures with 100 fixed courses and variable wale numbers.

By inserting the ratio of the four linear resistances into equations (18) and (22), the simulated and experimental results of the resistances with their error bars for different structures with 100 fixed wales and variable course numbers were obtained and are shown in Figure 23; the simulated and experimental results with their error bars of the resistances of different structures with 100 fixed courses and 10 pattern repeat units are shown in Figure 24. The reason for the collection of different data in the course and wales directions was explained in the preceding sample preparation section. The data points connected by solid lines are the simulation results, and those connected by dashed lines are the experiment results. To be clearly observed, enlarged images for the crowded sections framed by dashed rectangles in figure 23 (a) were graphed in figure 23 (b) to (e). It is evident that the trend of the two data sets is generally identical. It can also be observed that the experimental results coincide with the theoretical results within an acceptable degree of error in cases in which the conductive yarns are embedded in both the horizontal and vertical directions.

As shown in Figure 23, the resistance value is inversely proportional to the course

number of the conductive fabric. This result can be explained by Ohm's law, which states that a parallel connection will reduce the resistance of a circuit.

It can be seen from Figure 23 that the jersey structure has the largest resistance, followed by the 1x1, 1x2, 1x3, 1x4, and 1x5 float structures in descending order. The highest value recorded in the experiment was approximately 80  $\Omega$  and was associated with one course of conductive yarn knitted in the jersey structure. However, when the conductive yarn was knitted in five courses, the measured resistance value was very low, especially with float structures, which were all approximately 10  $\Omega$ . With an increase in the number of float stitches in a float structure unit, the resistance values tended to decrease because an increase in float stitches will generally increase the number of parallel conductive yarns in the structure, which helps to decrease the resistance. The resistance values will finally approach a marginal value as the float stitch number approaches infinity. This result occurs because the number of loop stitches is dramatically reduced because these stitches are replaced by float stitches when there is an increase in float stitches. Additionally, when there is an increase in knitting courses in a knitted fabric, the resistive effect will be diminished and, thus, the resistance values of the conductive knitted fabric with various numbers of knitting courses become similar. The reason is still that an increase in the number of parallel connections in a circuit reduces the overall resistance value.

The discrepancy illustrated in Figure 23 between the experimental and theoretical values can be explained by the instability of the knitted fabric. It can be seen that the experimental results are very close to the theoretical results for the jersey structure (i.e., when  $n=0$ ). Consistent with the increasing number of float stitches, the difference between the experimental and simulated results becomes more noticeable. The relatively large difference in the two sets of results occurs for the structures of the 1x4 and 1x5 floats. In the jersey fabric, the loop is arranged one by one tightly, the deformation of the loop is very limited, and the theoretical model fits the loop status well. Therefore, the variation between the experimental data and the simulated results is small. However, regarding the float structure, although the float yarn stitches are knitted under the same machine parameters as those used for the jersey structure, the loop shape has been changed under the influence of the float stitch in the fabrics because the embedded float yarn can make the knit stitch slightly looser than the knit

stitch in the jersey structure. Because the model of the float stitch is established based on the knit stitch in the jersey structure, there should be some deviation between the practical and theoretical results. However, the discrepancy is small and, thus, acceptable. An improved method could be developed by considering the loop deformation when establishing the model for float structures or when developing new knitting techniques to make the float structures as stable as the jersey structure.

In Figure 24, when repeat times and course numbers were both fixed, although the wales number varied among the different structures, the resistance value remained constant because the length of the float yarn did not influence the resistance values according to equation (22). However, the experimental values trended slightly upward, which was due to the existence of the electric current in the horizontal direction during the measurement of the resistance. The electric current in the horizontal direction was ignored in the calculations; however, such a current will indeed be generated when loading a voltage source due to the slight asymmetry at the edge of the resistive network. As the resistance of the float yarn increased, the resistance in the horizontal direction increased, which restrained the conduction of the electric current in the horizontal direction. Therefore, the final resistance was approximately constant with a slight increase.

## **Conclusion**

This paper presented a reasonable theoretical description of the resistance values of different knitted structures formed with knit and float stitches. The theoretical conclusions were well verified by the experimental values, and the deviation between the experimental and theoretical values can be explained reasonably well with the related electrical knowledge. It may be concluded that float stitches can definitely decrease the overall resistance of a conductive fabric compared with the resistance of a fabric with only knit stitches when the wales number is fixed. However, the changes in the float structure have little influence on the resistance of a knitted fabric when the course number is fixed. Considering these rules, when designing a conductive knitted fabric with specific resistance values, increasing the number of float stitches in one pattern unit could reduce the resistance of the overall fabric, and keeping the repeat number of pattern units unchanged could enlarge the fabric size with constant fabric

resistance. Therefore, this study provides an effective method for the computation of resistance values in a conductive knitted fabric. Simultaneously, it demonstrates the possibility of controlling the resistance values of a conductive knitted fabric of fixed dimensions and density. Moreover, the research provides a scientific method for a further research on contact resistance and length-related resistance in conductive knitted fabrics, which can also be adopted for the study of tuck structures in the future.

### **Declaration of conflicting interests**

The authors declared no potential conflicts of interest with respect to the research, authorship, and/or publication of this article.

### **Funding**

The authors disclosed receipt of the following financial support for the research, authorship, and/or publication of this article: This work was supported by the Research Grants Council (RRF) of Hong Kong, Ref No. 15403114 (PolyU154031/14H).

### **References**

1. Park S and Jayaraman S. *Smart textiles: Wearable electronic system*. Cambridge: Cambridge University Press, 2003.
2. Mattila HR. *Intelligent textiles and clothing*. Amsterdam: Woodhead Publishing, 2006.
3. Gregory RV, Kimbrell WC and Kuhn HH. Conductive textiles. *Synth Met* 1989; 28: 823–835.
4. Hassonjee QN, Cera J, Bartecki RM, et al. *Textile-based electrode*. Patent 7970451, USA, 2011.
5. Lin P and Yan F. Organic thin film transistors for chemical and biological sensing. *Adv Mater* 2012; 24: 34–51.
6. Lymberis A and Olsson S. Intelligent biomedical clothing for personal health and disease management: state of the art and future version. *Telemed J e-Health* 2003; 9: 379–386.
7. Gibbs PT and Asada HH. Wearable conductive fiber sensors for multi-axis human joint angle measurements. *J NeuroEng Rehabil* 2005; 2: 35–42.
8. Metcalf CD, Collie SR, Cranny AW, et al. Fabric-based strain sensors for measuring movement in wearable tele-monitoring applications. In: *IET*



*conference on assisted living*, 2009, pp.13–16.

9. Ceken F, Kayacan O, Ozkurt A, et al. The electro- magnetic shielding properties of some conductive knitted fabrics produced on single or double needle bed of a flat knitting machine. *J Text Inst* 2012; 103: 968–979.
10. Rock M and Sharma V. *EMI shielding fabric*. Patent 1330964, EP, 2011.
11. Sezgin H, Bahdir S, Boke YE, et al. Effect of different conductive yarns on heating behaviour of fabrics. In: *PMUTP international conference: textile & fashion*, 2012.
12. Liu K, Sun Y, Lin X, et al. Scratch-resistant, highly conductive, and high-strength carbon nanotube-based composite yarns. *ASCNANO* 2010; 4: 5827–5834.
13. Perez JS. *Heatable fabric coating*. Patent 2525625A1, EP, 2012.
14. Cherenack K, Zysset C, Kinkeldei T, et al. Woven electronic fibers with sensing and display functions for smart textiles. *Adv Mater* 2010; 22: 5178–5182.
15. Linz T, Kallmayer C, Aschenbrenner R, et al. Embroidering electrical interconnects with conductive yarn for the integration of flexible electronic modules into fabric. In: *ninth IEEE international symposium*, 2005.
16. Wever MO, Akter F and Ehrmann A. Shielding of static magnetic fields by textiles. *Ind Text* 2013; 64: 184–187.
17. Paradiso R, Loriga G and Taccini N. A wearable health care system based on knitted integrated sensors. *IEEE Trans Inform Technol Biomed* 2005; 9: 337–344.
18. Liu R, Wang S, Lao TT, et al. A novel solution of monitoring incontinence status by conductive yarn and advanced seamless knitting techniques. *J Eng Fibers Fabrics* 2012; 7: 50–56.
19. Li L, Au WM, Li Y, et al. Design of intelligent garment with transcutaneous electrical nerve stimulation function based on the intarsia knitting technique. *Text Res J* 2010; 80: 279–286.
20. Li L. *Innovative functional knitwear design with conductive yarn*. PhD Thesis, The Hong Kong Polytechnic University, 2010.
21. Li L, Au WM, et al. A novel design method for an intelligent clothing based on garment design and knitting technology. *Text Res J* 2009; 79: 1670–1679.
22. Li L, Liu S, et al. Electromechanical analysis of length- related resistance and contact resistance of conductive knitted fabrics. *Text Res J* 2012; 82: 2062–2070.
23. Li L, Au WM, et al. Wearable electronic design: electro- thermal properties of conductive knitted fabrics. *Text Res J* 2013; 84: 477–487.
24. Li L, Au WM, et al. Smart textiles: a design approach for garments using conductive fabrics. *Des J* 2014; 17: 137–154.
25. Qureshi W, Guo L, Peterson J, et al. Knitted wearable stretch sensor for breathing monitoring application. *Proc Ambience* 2011; 32: 72–76.
26. Ceken F, Pamuk G, Kayacan O, et al. Electromagnetic shielding properties of plain knitted fabrics containing conductive yarn. *J Eng Fibers Fabrics* 2012; 7: 81–87.
27. Syed TAH, Prasad P and Anura F. Thermo-mechanical behavior of textile heating fabric based on silver coated polymeric yarn. *Materials* 2013; 6: 1072–1089.
28. Zhang H, Tao XM, Yu TX, et al. Conductive knitted fabrics as large- strain gauge under high temperature. *Sens Actuators* 2006; 126: 129–140.

29. Yang K, Song GL, Zhang L, et al. Modelling the electrical property of 1x1 rib knitted fabrics made from conductive yarns. In: *Second international conference on information and computing science*, 2009, Vol.4, pp.382–385.
30. Li L, Au WM, Li Y, et al. A resistive network model for conductive knitting stitches. *Text Res J* 2010; 80:935–947.
31. Wang JF, Long HR, Soltanian S, et al. Electromechanical properties of knitted wearable sensors: part 1- theory. *TextRes J* 2014; 84: 3–15.
32. Wang JF, Long HR, Soltanian S, et al. Electromechanical properties of knitted wearable sensors: part 2- parametric study and experimental verification. *Text Res J* 2014; 84: 200–213.
33. Au KF. *Advances in knitting technology*. Amsterdam: Woodhead Publishing, 2011.
34. Perice FT. Geometrical principles applicable to the design of functional fabrics. *Text Res J* 1947; 17: 123–147.
35. Leaf GAV and Glaskin A. 43—the Geometry of a Plain Knitted Loop. *J Text Inst Trans* 1955; 46: T587–T605.
36. Munden DL. 26—the geometry and dimensional proper- ties of plain-knit fabrics. *J Text Inst Trans* 1959; 50:448–471.
37. Postle R. 17—A geometrical assessment of the thickness and bulk density of weft-knitted fabrics. *J Text Inst Trans* 1974; 65: 155–163.
38. Semnani D, Latifi M, Hamzeh S, et al. A new aspect of geometrical and physical principles applicable to the estimation of textile structures: an ideal model for the plain-knitted loop. *J Text Inst* 2003; 94: 202–211.
39. Haykin SS. *Active network theory*. London: Addison- Wesley, 1970.